International Journal of Fluid Power 1 (2000) No. 1 pp. 49-58

COMPUTERIZED GENERATION OF NOVEL GEARINGS FOR INTERNAL COMBUSTION ENGINES LUBRICATING PUMPS

G. Mancò [1, S. Mancò, M. Rundo [2, N. Nervegna

Dipartimento di Energetica, Politecnico di Torino, Corso Duca degli Abruzzi, 24 - 10129 Torino, Italy
[1State Technical Institute (ITC), Avezzano, Italy
[2Magneti Marelli SpA, Divisione Componenti Meccanici, Livorno, Italy
saman@polito.it, rundo@op94.polito.it, niner@polito.it

Abstract

The paper presents a general procedure for the computerized design of gerotor lubricating pumps for internal combustion engines. The approach is applied to gerotor gearings with circular arc profiles, nowadays the most used, but also to pumps featuring novel parabola arc profiles. Obtained results allow, on one hand, to guide the designer in selecting gerotor (circular arc) prototypes best suited for a given application and, on the other hand, to scrutinize novel profiles by the same generalized approach.

Keywords: lubricating pumps, gerotor, cycloidal gearings

1 Introduction

The continuous evolution of modern automotive engines sets stringent requirements on lubricating pumps in terms of specific displacement (referred to size), absorbed power and fluidborne noise. Over time, external and internal gear pumps have been replaced by more compact designs featuring Gerotor or Duocentric gearings, the latter warranting a 20% increase in displacement at equal size and number of teeth. Nevertheless, several problems are still open. As an example, practically all pumps exhibit low volumetric efficiencies at high rotational speeds owing to incomplete chambers filling. Consequently excessive fluidborne noise, fatigue and possible breakdowns may follow. A need then exists from the early stages of design, to cope with requirements set forth by the given application. Through the process of profiles generation, in concert with a general approach as proposed by Litvin (1994), Litvin (1996), one has to ascertain design parameters to comply with criteria regarding: (a) displacement and size; (b) gearings contact stresses and sliding velocity; (c) variable volume chambers filling. A high specific displacement pump permits to satisfy oil flow rate demand at hot idling conditions of the engine, by far the most critical. The impact of design parameters on gears contact stresses have been studied by Colbourne (1976): a change in gears proportioning through an increase of the minimum radius of curvature sensibly lowers contact stresses without putting a penalty on the yield in flow rate. However, since stresses also depend on the number of teeth, the generating circle radius and tolerances, the design phase must take these into account. The pump chambers filling process is basically influenced by volumes rate of change and it is then possible to screen specific profiles that, other conditions being the same, lead to more favourable volume variation rates. This paper will detail a generalized procedure for the generation of gerotor pump profiles meeting all cited requirements. At first the methodology will be applied to the well known circular pin gear profiles and, then, by way of example, to a new gear profiles family originated by parabolic pin. This, hopefully, will open the way to identify new prototypes of lubricating pumps worth of further investigations involving simulation as well as experimental analyses.

This manuscript was received on 7 December 1999 and was accepted after revision for publication on 9 February 2000

2 Circular Pin Gear Profile Generation

Consider two gears rotating in the same direction about parallel axes O_1 and O_2 at a constant ratio of angular velocities $\omega^{(1)}$ and $\omega^{(2)}$. The gears differ by one in their number of teeth (gerotor) and their centrodes are circles, of radii r_1 and r_2, in internal tangency. Coordinate systems S_1 (O_1, x_1, y_1, z_1), S_2 (O_2, x_2, y_2, z_2)

and (S_f , O_f, x_f , y_f , z_f) are rigidly connected to the external gear (body 1), the internal gear (body 2) and the pump casing, respectively (Fig. 1).

2.1 Internal Gear Profile Σ_2

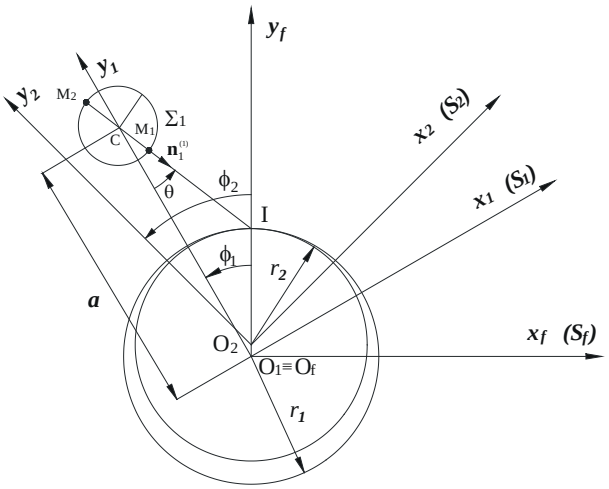

Fig. 1: *Generation of trochoidal curves with circular arcs*

Let us consider a cycloidal profile (trochoid), generated in the coordinate system S_2 by a pin circle Σ_1 centered in C with radius ρ, rigidly connected to S_1. Point I is the instantaneous center of rotation. The trochoid curve Σ_2 conjugated with the generating circle Σ_1 must be determined in the interval $\phi = 2\pi / N_1$, being N_1 the number of generating pins and ϕ the rotational angle of the gear with which pins are rigidly connected, i.e., $\phi = \phi_1$. Using homogeneous coordinates the position vector of point M_1 of the generating pin Σ_1 is (Fig. 1):

$$r_1(\theta) = (M_1 - O_1') = \left[\rho \sin\theta \quad a - \rho\cos\theta \quad 0 \quad 1\right]^T \qquad (1)$$

The superscript T means that $[r_1(\theta)]^T$ is a transpose matrix with respect to $\boldsymbol{r}_1(\theta)$. By coordinate transformation from S_1 to S_2 we have:

$$r_2(\theta,\phi) = (M_1 - O_2) = M_{21}(\phi) r_1(\theta) \qquad (2)$$

where matrix $\boldsymbol{M}_{21}$ performs a co-ordinate transformation from S_1 to S_2 and $e = r_1 - r_2$ is the eccentricity, i.e. the distance separating centers O_1 and O_2 .:

$$M_{21}(\theta) = \begin{bmatrix} \cos(\phi_1 - \phi_2) & -\sin(\phi_1 - \phi_2) & 0 & -e\sin\phi_2 \\ \sin(\phi_1 - \phi_2) & \cos(\phi_1 - \phi_2) & 0 & -e\cos\phi_2 \\ 0 & 0 & 1 & 0 \\ 0 & 0 & 0 & 1 \end{bmatrix} \qquad (3)$$

To determine the internal gear profile an additional equation is needed to relate angle θ, describing the generating circle, and angle the generalized parameter of motion, i.e., the equation of meshing. There are three alternative approaches for the derivation of the equation of meshing, Litvin (1996):

- (applied in differential geometry) The rank of the Jacobian matrix formed with the first derivatives of $\boldsymbol{r}_2$ (θ, ϕ) with respect to θ and ϕ is one.
- (in theory of gearing) The normal component value of the sliding velocity vector in relative motion is zero, i.e. the sliding velocity is tangent to the internal gear profile Σ_2
- (based on Lewis' theorem) The normal to pin circle Σ_1 at the point of tangency of Σ_1 and Σ_2 passes through the instantaneous centre of rotation I. Regardless of the choice one arrives at the following equation of meshing:

$$f(\theta,\phi) = r_1 \sin(\theta + \phi) - a\sin\theta = 0 \qquad (4)$$

From Eq. (4) angle θ can be expressed as a function of the generalized parameter of motion ϕ:

$$\tan\theta = \frac{\sin\phi}{\lambda - \cos\phi} \quad \text{with} \quad \lambda = \frac{a}{r_1} \qquad (5)$$

and by insertion in $\boldsymbol{r}_1$ allows the determination of $\boldsymbol{r}_2$. Worth of note is the fact that Eq. (5) provides two solutions for values of θ differing by 180°. This conforms to points M_1 and M_2 of Fig. 1. What matters here is the interior point (M_1), whereby the working portion of the generating pin is a circular arc swept back and forth by the contact point M_1.

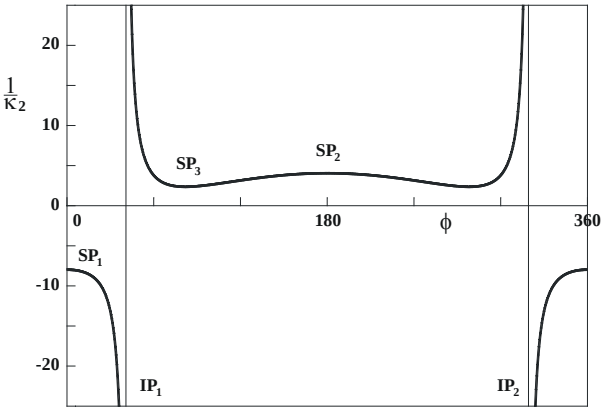

Fig. 2: *Inflection and stationary points of curvature radius for the internal gear profile generated with pin circles a = 34.75 mm, ρ = 7.5 mm, e = 2.2 mm = N_1 = 11*

Curvature of Σ_2. The curvature κ_2 of curve Σ_2 can be represented, Litvin (1996), with the sign convention that curvature radius is negative, if curve κ_2 is convex and positive if concave, by the equation

$$\frac{1}{\kappa_2} = -\frac{r_1(\tau_{21} - 1)(\lambda^2 - 2\lambda\cos\phi + 1)^{3/2}}{-(\tau_{21} - 1)\lambda^2 - \tau_{21} + (2\tau_{21} - 1)\lambda\cos\phi} - \rho$$

where

$$\tau_{21} = \frac{N_1}{N_2} = \frac{N_1}{N_1 - 1} = \frac{\omega^{(2)}}{\omega^{(1)}} = \frac{r_1}{r_2} = \frac{\phi_2}{\phi_1} \quad \text{and} \quad \lambda = \frac{a}{r_1} \qquad (6)$$

Figure 2 shows the curvature radius of the inner rotor of a commercially available lubricating pump.

Inflection Points: IP. Points of the trochoidal curve Σ_2 where $\frac{1}{\kappa_2} \to \infty$ qualify as inflection points (see points IP in Fig. 2). Traversing inflection points a sign change is observed in the curvature radius. By enforcing the existence of inflection points, so that a regular

sequence of concave-convex branches in the gear profile is obtained, values of λ must be constrained as follows:

$$1 \le \lambda \le \frac{\tau_{21}}{\tau_{21}-1} = N_1 \tag{7}$$

Stationary points: SP. These are identified on the internal gear profile Σ_2 under the circumstance of maxima or minima values of the curvature radius, that is, when:

$$\frac{\mathrm{d}}{\mathrm{d}\phi}\left(\frac{1}{\kappa_2}\right) = \sin\phi\left[\left(2-\tau_{21}\right)\lambda^2 + \left(2\tau_{21}-1\right)\lambda\cos\phi - \left(\tau_{21}+1\right)\right] = 0 \tag{8}$$

From Eq. (8) stationary points on Σ_2 (points *SP* in Fig. 2) are identified at locations determined through the following relations:

$$\sin\phi = 0 \quad \text{and} \quad \cos\phi = \frac{\left(\tau_{21}-2\right)\lambda^2 + \tau_{21} + 1}{\left(2\tau_{21}-1\right)\lambda} \tag{9}$$

Singularities of Σ_2. The normal to the generated curve Σ_2 at a singular point is undefined and at that point Σ_2 may exhibit two branches. Singular points are therefore not admissible and should be avoided by proper selection of design parameters. A singular point on Σ_2 occurs if the relative velocity $\boldsymbol{v}_r^{(2)}$ of the contact point becomes zero. Since $\boldsymbol{v}_r^{(2)}$ is the vector sum of the contact point velocity relative to Σ_1 and the profiles sliding velocity, the above condition may be written as:

$$v_r^{(2)} = v_r^{(1)} + v^{(12)} = 0 \tag{10}$$

that leads to:

$$\left(a - \rho\cos\theta - r_1\cos\phi\right)\left(\tau_{21}-1\right) + \rho\cos\theta\frac{\mathrm{d}\theta}{\mathrm{d}\varphi} = 0 \tag{11}$$

This, together with (4), the equation of meshing, allows determination of boundaries for ρ to avoid singularities on Σ_2. These are so expressed:

$$-\frac{r_1\left(\tau_{21}-1\right)\left(\lambda-1\right)^3}{\lambda^2\left(1-\tau_{21}\right)-\tau_{21}+\left(2\tau_{21}-1\right)\lambda} \le \rho \le \frac{\left(\tau_{21}-1\right)\sqrt{27\left(a^2-r_1^2\right)}}{\left(2\tau_{21}-1\right)^{3/2}} \tag{12}$$

When ρ equals either limits the radius of curvature $1/\kappa_2$ becomes zero in coincidence with stationary points. Outside this range and within the portion delimited by the two inflection points $IP_1$and IP_2, a sign change is observed in $1/\kappa_2$ and the profile is no more regular.

2.2 External Gear Profile Σ_1'

The external gear profile Σ_1' is the envelope of Σ_2 swept in S_1

$$r_1\left(\theta,\phi,\psi\right) = M_{12}\left(\psi\right)r_2\left(\theta,\phi\right) \tag{13a}$$

together with

$$f\left(\theta,\phi\right) = r_1\sin\left(\theta+\phi\right) - a\sin\theta = 0 \tag{13b}$$

Angles $\psi_1 = \psi$ and $\psi_2 = \tau_{21}\psi_1$ represent rotation angles of Σ_2 and Σ_1 about their respective centres O_2 and O_1 .

The co-ordinate transformation matrix $M_{12}(\psi)$ is similar to $M_{12}(\phi) = M_{21}^{-1}(\phi)$ where $\phi = \psi$.

Based on the equation of meshing between Σ_2 and Σ_1 derived using one of the three alternative approaches mentioned previously:

$$F\left(\theta,\phi,\psi\right) = \sin\left(\theta+\phi_1-\phi_2+\psi_2\right) - \sin\left(\theta+\phi_1\right) = 0 \tag{14}$$

two solutions can be obtained for ψ_2 corresponding to the two branches of the envelope Σ_1' :

$$\begin{aligned} \bar{\psi}_2 &= \phi_2 + 2\pi\cdot m \\ \bar{\psi}_2' &= \phi_2 + \left(2m+1\right)\pi - 2\left(\theta+\phi_1\right) \end{aligned} \tag{15}$$

where m = 0, 1, 2, ..., N_1-1

2.3 Line of Contact

At every instant, the mating gear profiles are in contact along a path called the contact line. This path may be thought of as the trace of contact points of the external gear as seen by an observer fixed to co-ordinate system S_f (see Fig. 1):

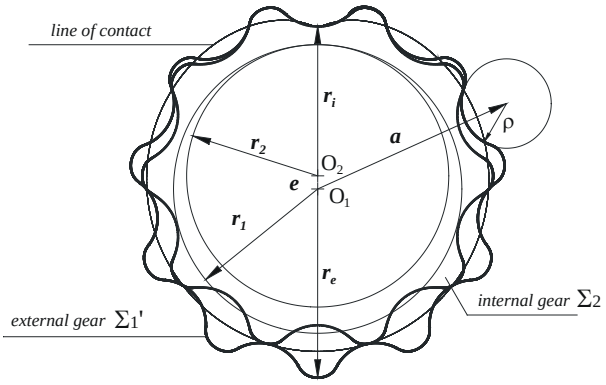

Fig. 3: *Profiles and geometric parameters of gearings*

$$r_f\left(\theta,\phi\right) = M_{f1}\left(\phi\right)r_1\left(\theta\right) \tag{16}$$

where M_{f1} is the transformation matrix:

$$M_{f1}\left(\phi\right) = \begin{bmatrix} \cos\left(\phi\right) & -\sin\left(\phi\right) & 0 & 0 \\ \sin\left(\phi\right) & \cos\left(\phi\right) & 0 & 0 \\ 0 & 0 & 1 & 0 \\ 0 & 0 & 0 & 1 \end{bmatrix} \tag{17}$$

Complying with conditions (7) and (12) it is feasible to generate gerotor gearings of any size that show a correct meshing (Fig. 3).

2.4 Gears Design Criteria

However, the search for gearings design parameters appropriate to a specific applications remains too extensive. Fixing the number of teeth of the external gear N_1, three quantities need still be defined to arrive at a complete characterization of the gearing and precisely α, ρ and e. An additional condition must be stated to complement inequalities (7) and (12). Since in gerotor lubricating pumps the outside diameter of the external gear is often constrained, the missing condition can be

so written (Fig. 3):

$$r_e = a - \rho + 2 \cdot e \tag{18}$$

Things so standing, the problem can be phrased as follows: given N_1 and r_e, find α, ρ and e on grounds of conditions (7), (12) and (18). As an example, consider the case of a pump with N_1 = 11 and r_e = 32 mm. Fig. 4 shows compatible intervals of the three parameters as functions of $\lambda = a/r_1$. Black dots indicate values selected for the lubricating pump of the Fire 1200 engine, Fabiani (1998). Considering that the problem has different and feasible solutions, further constraints must be exercised to arrive at an optimal design of the gearings.

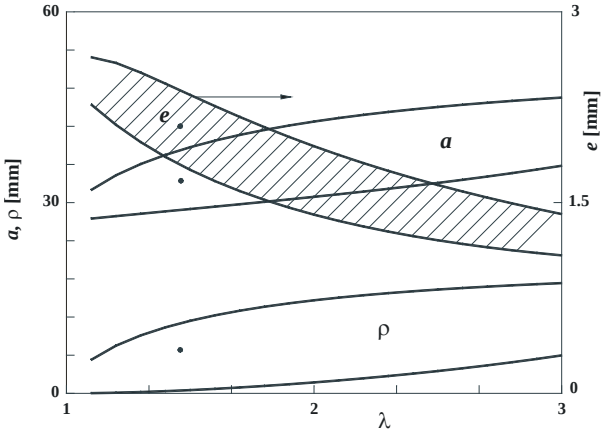

Fig. 4: *Admissible ranges of design parameters for a gearing with N_1 = 11 and r_e = 32* mm

Criteria reflex-ive of specific practical requirements are based on:

- displacement -> flow rate;
- sliding velocity -> wear of materials;
- kinematic flow ripple -> fluidborne noise;
- variable volume chambers filling -> air release and cavitation -> airborne noise;
- contact stresses -> wear of materials.

Profiles sliding velocity can be evaluated as follows, Litvin (1994), Litvin (1996):

$$\nu_1^{(12)} = \omega_1^{(1)} \left(\tau_{21} - 1\right) \begin{bmatrix} a - \rho\cos\theta - r_1\cos\phi \\ -\rho\sin\theta + r_1\sin\phi \\ 0 \end{bmatrix} \tag{19}$$

$$\nu_s = \left|\nu_1^{(12)}\right| \tag{20}$$

The maximum admissible value of sliding velocity can be procured from manufacturing data of commercial pumps.

Kinematic flow ripple can be determined from the ideal flow rate of the pump consequent to chambers volumes rate of change:

$$Q = -\omega_1^{(2)} \sum_1^n \frac{\mathrm{d}V}{\mathrm{d}\phi} \tag{21}$$

where n is the number of chambers simultaneously connected to delivery (ideal port timing being assumed). As a measure of flow fluctuations a flow ripple index is introduced, defined in the usual way:

$$\varepsilon = \frac{Q_{\max} - Q_{\min}}{Q_{av}} \tag{22}$$

Volume variations can be expediently evaluated via the vector rays method, Fabiani (1998). Vector rays connect gears centres with profiles contact points: the net volume variation of each chamber, given by the area change multiplied by gears thickness H, comes from the summation of individual contributions of the two rotors. With reference to volumes V_i and V_e in Fig. 5 we have:

$$\frac{\mathrm{d}V}{\mathrm{d}\phi} = \frac{\mathrm{d}V_e}{\mathrm{d}\phi} + \frac{\mathrm{d}V_i}{\mathrm{d}\phi}$$

$$\frac{\mathrm{d}V}{\mathrm{d}\phi} = \frac{1}{2} H \left\{ \left[\left(\rho_A^{(1)}\right)^2 - \left(\rho_B^{(1)}\right)^2 \right] + \left[\left(\rho_B^{(2)}\right)^2 - \left(\rho_A^{(2)}\right)^2 \right] \tau_{21} \right\} \tag{23}$$

Knowing the derivative (23), integration yields chamber volume and thus displacement. The accuracy of the method is high and it is addressed elsewhere, Fabiani (1998). As to chambers filling, writing the momentum equation in the axial direction of the chamber, it is possible to evaluate the pressure drop required to achieve its complete filling, Singh (1991), Mancò (1999).

$$\Delta p_{\max} = \rho(\omega_1^{(2)} \cdot H)^2 \cdot \left(\frac{\mathrm{d}V / \mathrm{d}\phi}{V(\phi)} \right)^2 \tag{24}$$

with ρ = oil density

Equation (24) highlights the fact that when $V(\phi)$, or more precisely, the flow area, is small, pressure drop Δp_{max} climbs to very high values, this occurring at the beginning as well as at the end of the suction phase. One simplifying hypothesis that has been made lies in assuming the minimum chamber volume as being a constant fraction (2.5%) of displacement.

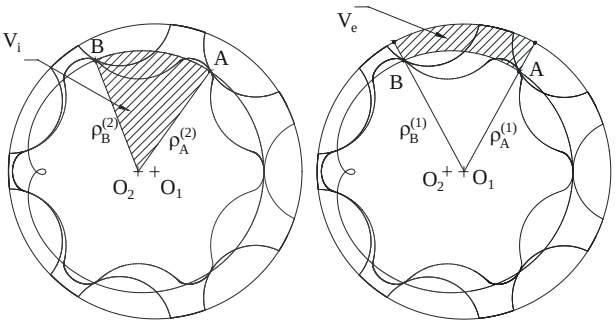

Fig. 5: *Vector rays for the evaluation of volume variations*

Contact stresses have been studied, among others, by Colbourne (1976). Most influential parameters were shown to be the operating pressure, the number of teeth and the minimum radius of curvature of the internal gear. Owing to the fact that for lubricating pumps oil pressure is relatively low, contact stresses should not be of concern. For this reason only the minimum radius of curvature ρ_{min} (that should preferably be high) has been accounted as a decision variable in gearings design.

2.5 Calculated Results

Fig. 6 shows a collection of admissible ranges for design decision variables of a gerotor pump

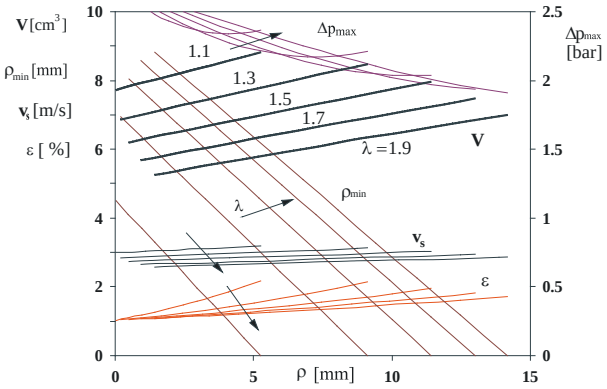

Fig. 6: *Influence of design parameters of a pin circle gerotor gearing with N_1 = 11 and r_e = 32 mm on displacement V, flow ripple index ε, profiles sliding velocity v_s, minimum radius of curvature of the internal gear profile ρ_{min}, and vane filling capacity Δp_{max} (right axis) versus circular pin radius at constant λ*

featuring N_1 = 11, and r_e = 32 mm gears thickness H = 10 mm. For the calculation of Δp_{max} and v_s a maximum internal gear angular speed of $\omega_2 = 200\pi$ rad/s has been considered, i.e., the same of the engine if the pump is crankshaft mounted. Data are plotted as functions of ρ and $\lambda = a/r_1$.

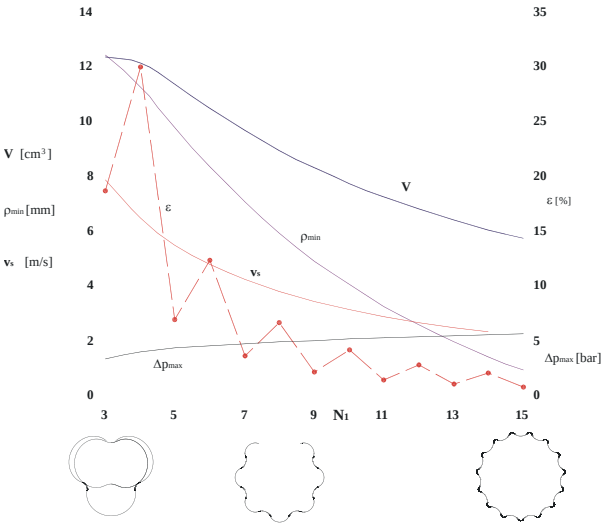

Fig. 7: *Displacement, ρ_{min}, sliding velocity v_s (left axis) and ε, Δp_{max} (right axis) versus number of teeth in external gear with λ=1.5, ρ / r_1 = 0.3, r_e 32 mm =*

Of relevance is the fact that, at constant λ, displacement increases almost linearly with ρ but, at constant ρ, decreases as λ is increased. These outcomes are only in partial agreement with those published by Beard (1985), Beard (1989). In fact, varying the radius of the generating circle at a given λ, $1.2 \le \lambda \le 6$, Beard (1989) found that the influence on flow and displacement is minimal (less than 1%). Conversely in Beard (1985) a confirmation is given of a decrease in displacement when λ is increased. Sliding velocity and flow ripple behave as displacement: both increase with ρ but lessen with λ. An opposite behaviour is found for the minimum radius of curvature of the internal gear ρ_{min} and the pressure drop needed to assure complete filling of chambers. In fact, both decrease as ρ is increased, yet, at constant ρ, both increase with λ. The influence of another design parameter, i. e., the number of pumping elements N_1 is brought to evidence in Fig. 7, where, for given size r_e, λ and the ratio ρ / r_1, N_1 has been varied from 3 to 15. Although Fig. 7 is bound to explicit numerical values for the three parameters, trends being shown partake of generality.

- Displacement *V*. The falling off of pump displacement as the number of variable volume chambers is increased is clearly evident.
- Minimum radius of curvature ρ_{min}. Even sharper is the drop in the minimum radius of curvature of the internal gear profile with N_1, this being somewhat alleviated by the fact that a higher number of teeth (reasonably one half) are in mesh and share the total load.
- Profiles sliding velocity v_s. This becomes higher the lower is the number of teeth and reaches severe values at the low end of the range (rotational speed of 6000 rpm and crankshaft mounted internal gear).
- Flow ripple index ε. As mentioned earlier in the paper an ideal timing has been considered in the appraisal of instantaneous flow contributions to delivery. One then typically observes lower irregularities in connection with an odd number of chambers and at the same time a clear cut tendency towards a progressive reduction in flow ripple index as the number of chambers is increased (in the limit $\varepsilon \to 0$ as $N_1 \to \infty$). However, simulation analyses, Rundo (1996-1998), Mancò (1999), have shown that, due to account being taken of real timing and porting, oil compressibility and leakages, the advantage of odd vs even chambers in providing lower irregularities is not so apparent.
- Chamber filling potential Δp_{max}. In this respect, a meaningful parameter is the maximum pressure drop required to provide adequate filling at the highest pump speed. As the number of chambers is increased, filling becomes progressively more problematic, this being endorsed by specific in depth investigations, Mancò (1999).

An advantage of gerotor lubricating pumps, as opposite to external gear units, lies in the possibility of their direct mounting on the IC engine shaft. However, this entails an additional constraint in gearing design. In fact, beside the external space limit typified by r_e, an internal one expressed by r_i (see Fig. 3) must also be accounted as determined by the IC engine shaft dia-meter as well as by dimensions associated with the inner rotor alignment and sealing of pressurized chambers. The external radius of the external gear r_e and the internal radius of the internal gear r_i are correlated as follows (Fig. 3)

$$r_i = r_e - 3 \cdot e \tag{25}$$

This, inserted in (18), leads to a diverse and possibly more restrictive upper boundary, than that expressed in (12), for the ratio:

$$\frac{\rho}{r_1} \le \lambda - \frac{1}{N_1}\left(\frac{3r_i}{r_e - r_i} + 1\right) \qquad (26)$$

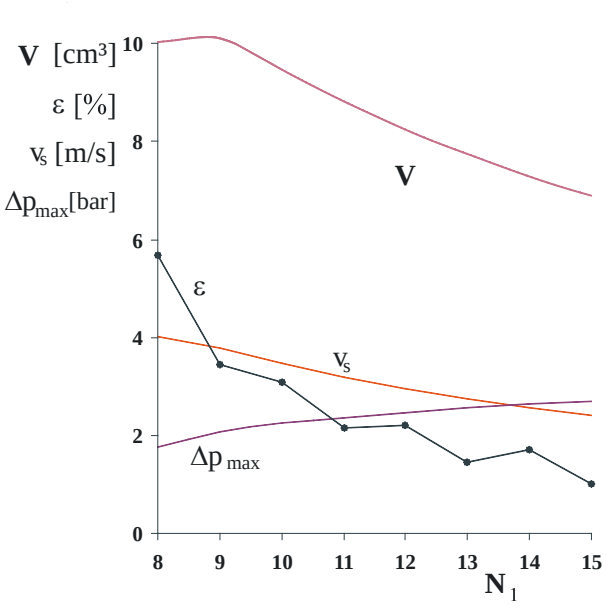

Fig. 8: *r_e=32 mm, r_i=22.5 mm, and maximum displacement*

Reasoning as in preceding examples, the case is now considered of a pump unit that must comply with the following, more restrictive, specifications: r_e=32 mm and r_i=22.5 mm. Aiming at maximizing displacement, Fig. 8 shows attainable results based on the number of chambers in the gearing. Since gears possessing less than 8 chambers do not fulfill the space requirement these have not been reported. When the number of chambers exceeds 9 the constraint due to the internal diameter is not influential.

3 Parabola Arc Gear Profiles Generation

This analysis is grounded on Fig. 9, similar to Fig. 1, with the exception of the pin circle being replaced by a parabolic pin. In polar co-ordinates the equation of the parabola with parameter and focus $F \equiv (0, a)$ is (see enlarged detail at left in Fig. 9):

$$\overline{FP} = r = \frac{2p}{1+\cos\theta} \qquad (27)$$

3.1 Internal Gear Profile Σ_2

In co-ordinate system S_1 the parametric equation of the parabola pin is:

$$r_1(\theta) = \left[2p\tan\frac{\theta}{2} \quad a - p + p\tan\frac{\theta}{2} \quad 0 \quad 1\right]^T \qquad (28)$$

The angle that the unit normal $\boldsymbol{n}_1^{(1)}$ forms with polar axis is θ/2, anticlockwise rotation is assumed positive. Point *P*, point *N* [with co-ordinates 0, *y* + 2 *p*): intersection of the normal to the parabola at point *P* with polar axis] and the centre of curvature *C* are all aligned and belong to the normal at point *P*. The fourth point in line: $I \equiv (r_1 \sin\phi, r_1 \cos\phi)$ is the instantaneous centre of rotation.

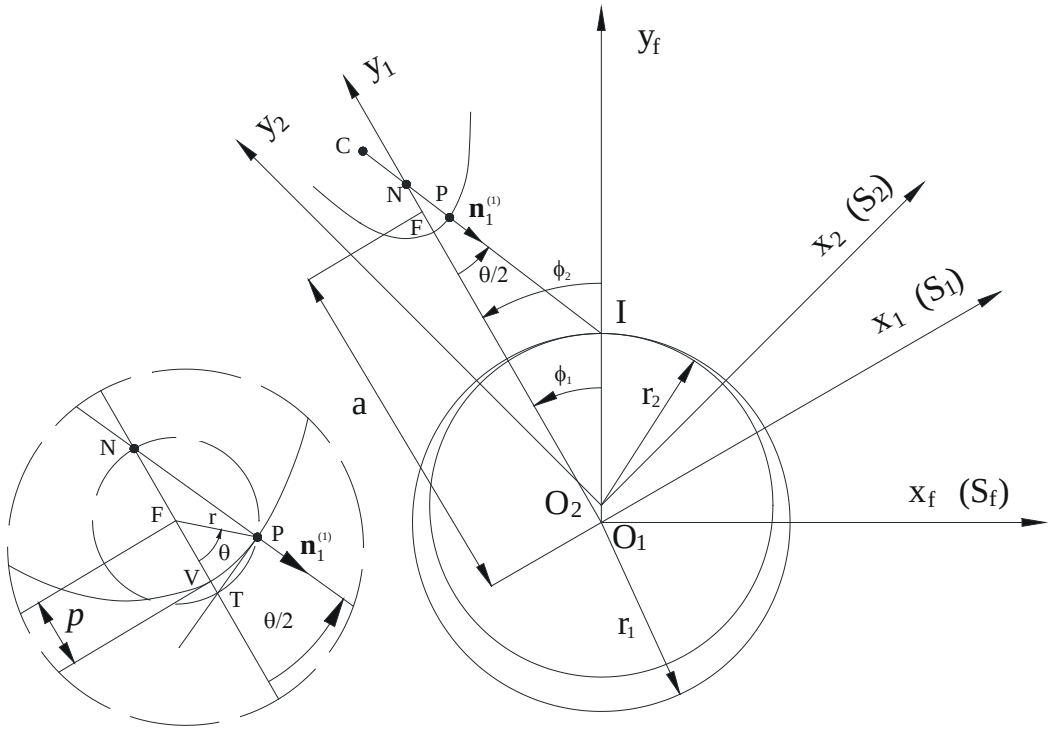

Fig. 9: *Generation of trochoid curves with parabola arcs (at left an enlarged view of the parabolic pin)*

It is possible to obtain the equation of meshing considering that the projection of sliding velocity on the normal must be zero, i.e.:

$$n_1^{(1)} \cdot v_1^{(12)} = 0 \tag{29}$$

The equation of the unit normal to the parabola at point *P* is:

$$n_1^{(1)} = \frac{N}{|N|} = \sin\frac{\theta}{2} i_1 - \cos\frac{\theta}{2} j_1 \tag{30}$$

since the normal to the parabolic pin is:

$$N = T \times k = \frac{p \sin\frac{\theta}{2}}{\cos^3\frac{\theta}{2}} \cdot i - \frac{p}{\cos^2\frac{\theta}{2}} \cdot j$$

where

$$N = T \times k = \frac{p \sin\frac{\theta}{2}}{\cos^3\frac{\theta}{2}} \cdot i - \frac{p}{\cos^2\frac{\theta}{2}} \cdot j \tag{31}$$

The sliding velocity of the mating surfaces Σ_1 and Σ_2 in the contact point can be calculated in the co-ordinate system S_1 as follows :

$$\begin{aligned} v_1^{(12)} &= \left[\omega_1^{(1)} - \omega_1^{(2)}\right] \times r_1 - \bar{O}_1\bar{O}_2 \times \omega_1^{(2)} \\ &= \omega_1^{(1)}\left(\tau_{21} - 1\right) \begin{bmatrix} a - p + p\tan^2\frac{\theta}{2} - r_1\cos\phi \\ -2p\tan\frac{\theta}{2} + r_1\sin\phi \\ 0 \end{bmatrix} \end{aligned} \tag{32}$$

Applying Eq. (29) it is possible to obtain the equation of meshing:

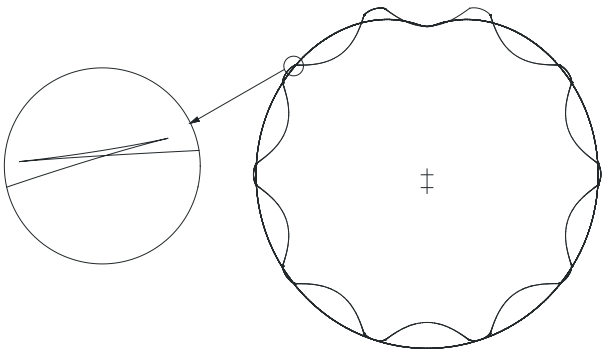

Fig. 10: *Line of contact and profile of the internal gear generated with parabolic arcs.* N_1*=11, a=31.71* mm, *p=4* mm, r_e*=32* mm *(at left an enlarged view of profile singularity)*

$$p\tan^3\frac{\theta}{2} + \left(a - r_1\cos\phi + p\right)\tan\frac{\theta}{2} - r_1\sin\phi = 0 \tag{33}$$

that leads to express θ as a function of φ:

$$\theta = -2a\tan\left\{\frac{\sqrt[3]{2}\delta}{\sqrt[3]{2\beta + \sqrt{\gamma}}} - \frac{\sqrt[3]{2\beta + \sqrt{\gamma}}}{3p\sqrt[3]{2}}\right\} \tag{34}$$

where

$$\delta = a + p - r_1\cos\phi;$$
$$\beta = 27p^2 r_1 \sin\phi$$

and

$$\gamma = 108p^3\delta^3 + 729p^4 r_1^2 \sin^2\phi$$

This, coupled to an equation similar to Eq. (2), permits to determine the internal gear profile (Fig. 10).

3.2 Curvature of Σ_2

The curvature of the generated profile can be expressed as in Litvin (1994):

$$\kappa_2 v_r^{(2)} = -\dot{n}_r^{(2)} \tag{35}$$

being, respectively, $\boldsymbol{v}_r^{(2)}$ and $\dot{n}_r^{(2)}$ the relative velocities on Σ_2 of the contact point and of the tip of the unit normal**.**

The relative velocity of the contact point on Σ_1 in the co-ordinate system S_1 is:

$$v_{r_1}^{(1)} = \dot{r}_1(\theta) = \frac{2p}{\cos^3\frac{\theta}{2}} \begin{bmatrix} \cos\frac{\theta}{2} \\ \sin\frac{\theta}{2} \end{bmatrix} \cdot \frac{1}{2}\frac{d\theta}{dt} \tag{36}$$

while the velocity of the same contact point on Σ_2 is equal to the sum of relative velocity on Σ_1 and sliding velocity:

$$v_r^{(2)} = v_r^{(1)} + v^{(12)} \tag{37}$$

In effect, to the end that contact continuity be preserved between gears, the absolute velocity of the point of contact must be the same for both gears:

$$v^{(abs)} = v_r^{(1)} + v_{tr}^{(1)} = v_r^{(2)} + v_{tr}^{(2)} \tag{38}$$

and hence

$$v_r^{(2)} = v_r^{(1)} + v_{tr}^{(1)} - v_{tr}^{(2)} = v_r^{(1)} + v^{(12)} \tag{39}$$

By insertion of Eq. (36) and (32) into Eq. (37) we obtain:

$$\begin{aligned} v_{r_1}^{(2)} &= \frac{2p}{\cos^3\frac{\theta}{2}} \left[\frac{1}{2}\frac{d\theta}{dt} + \omega_1^{(1)} - \omega_1^{(2)}\right] \begin{bmatrix} \cos\frac{\theta}{2} \\ \sin\frac{\theta}{2} \end{bmatrix} \\ &+ \omega_1^{(1)}\left(\tau_{21} - 1\right) \begin{bmatrix} a - r_1\cos\phi + p + 3p\tan^2\frac{\phi}{2} \\ r_1\sin\phi + 2p\tan^3\frac{\theta}{2} \end{bmatrix} \end{aligned} \tag{40}$$

By analogous reasoning, the velocity of the unit normal to the contact point in the co-ordinate system relative to the internal gear can be evaluated in S_1:

$$\dot{n}_r^{(2)} = \dot{n}_r^{(1)} + \omega^{(12)} \times n = \left[\frac{1}{2}\frac{d\theta}{dt} + \omega^{(1)} - \omega^{(2)}\right]\begin{bmatrix}\cos\frac{\theta}{2}\\ \sin\frac{\theta}{2}\end{bmatrix} \quad (41)$$

where the time derivative of θ stems from differentiation of the equation of meshing (33).

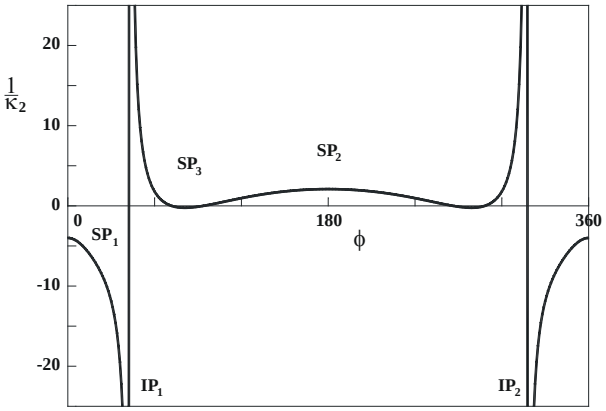

Fig. 11: *Inflection and stationary points on the curvature of the internal gear generated through parabola arcs: a=31.35* mm, *p=3.75* mm, *e=2.2* mm, $N_1=11$

Applying Rodrigues formula (35) we obtain the radius of curvature of the internal gear:

$$\frac{1}{\kappa_2} = -\frac{2p}{\cos^3\frac{\theta}{2}} - (\tau_{21}-1)\cdot\frac{a+p+3p\tan^2\frac{\theta}{2} - r_1\cos\phi}{\left[\frac{r_1\left(\cos\phi - \sin\phi\tan\frac{\theta}{2}\right)\cos^2\frac{\theta}{2}}{a+p+3p\tan^2\frac{\theta}{2} - r_1\cos\phi} + (1-\tau_{21})\right]\cos\frac{\theta}{2}} \quad (42)$$

The plot of the radius of curvature $1/\kappa_2$ (Fig. 11) appears similar to that shown earlier in this paper (Fig. 2). However, in this instance the circumstance is highlighted where, purposely, a negative stationary point SP_3 occurs consequent to specific proportioning. A singularity is therefore present along the profile (see Fig. 10).

3.3 Calculated Results

By the same line of reasoning as applied for circular arc profiles and following identical proportioning (as stated in Fig. 6) and evaluation criteria, results shown in Fig. 12 have been obtained. These are only marginally surprising. In fact, Colbourne (1976) has analysed circular, elliptic and sinusoidal generating curves deciding that the teeth shape has only a minor influence on the flow rate of ensuing pumps. Conversely, Fig. 12 brings to evidence displacement values sensibly smaller than those shown in Fig. 6. This leads to the conclusion that precise constraints do exist for the generating curve with respect to the attainable displacement.

However, if one proceeds from the specification of a definite target displacement, the evaluation of the remainder of decision variables (e.g. the flow ripple index, the chambers filling potential) could lead towards unconventional solutions.

4 Conclusions

The paper addressed the generation of gerotor gearings profiles for automotive engines lubrication pumps, even if, *inter alia*, the presented methodology applies, as well, to all gerotor and, with minor modification, orbit units.

Beside profiles generated by circular pins, the case of parabolic pins has also been considered. Results have proved that parameters selected for pump evaluation, and primarily displacement, are sensitive to the kind of generating pin. In more detail a factual su-

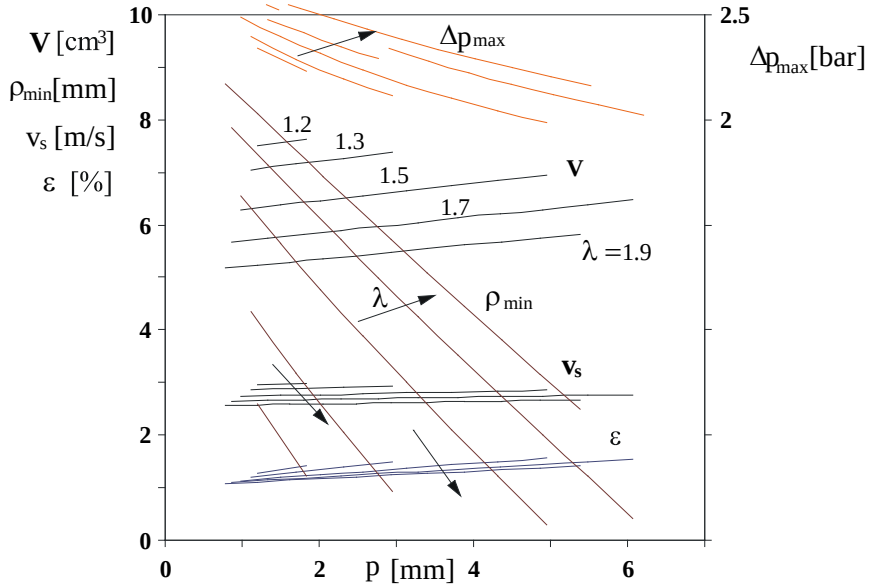

Fig. 12: *Influence of design parameters of a parabolic arc gerotor gearing with* $N_1=11$ *and* $r_e=32$ *[*mm*] on displacement V, flow ripple index ε, profiles sliding velocity* v_s*, minimum radius of curvature of the internal gear profile* ρ_{min}*, and vane filling capacity* Δp_{max}*, as function of p, focus to vertex distance in the pin.*

periority emerged for currently adopted profiles, i.e. circular generating pin.

The procedure is straightforward and applicable to other and novel profiles permitting to progress with inquiries aimed at the achievement of possibly better performance. Moreover, remaining at the current scenario of circular arc pumps, it also qualifies as a suitable guide for sorting out proper parameters for new prototypes deserving specific and more in depth researches granted from simulation and testing.

Nomenclature

a	distance of pin circle Σ 1 center (Fig. 1) or of pin parabola fo $\omega_i^{(12)}$ cus (Fig. 9) from O 1
$\Delta p_{\max}$	maximum pressure drop required to achieve complete chamber filling
e	eccentricity, the shortest center distance between body 1 and body 2
H	gears thickness
$\boldsymbol{M}_{ij}$ (ϕ)	coordinate transformation matrix from S *j* to S *i*
$\boldsymbol{N}$	Normal vector to Σ 1 in S 1
$\dot{\boldsymbol{n}}_r^{(j)}$	relative velocity of unit normal to profile Σ *j*
N_i	number of teeth of the external (i=1) or internal (i=2) gear
$\boldsymbol{n}_i^{(1)}$	unit normal to Σ 1 in coordinate system S *i*
O_i	origin of coordinate system S *i*
p	parameter in parabolic pin definition: focal distance from vertex (Fig. 9)
Q	ideal volumetric flow rate
$Q_{\max}$	maximum value of instantaneous flow rate
$Q_{\min}$	minimum value of instantaneous flow rate
Q_{av}	mean value of instantaneous flow rate
r_i	radius of centrode of external gear (i=1) and internal gear (i=2)
$\boldsymbol{r}_i$	position vector of profile Σ *i* in S *i*
r_e	outer radius of the external gear (Fig. 3)
r_i	inner radius of the internal gear (Fig. 3)
S_i	coordinate system fixed to the external (*i* = 1) or internal (*i* = 2) gear or pump case (*i* = *f*) .
$\boldsymbol{T}$	tangent vector to Σ 1
V	pump displacement
$\boldsymbol{v}^{(12)}$	profiles sliding velocity
$\boldsymbol{v}^{(abs)}$	point of contact absolute velocity
V(ϕ)	variable chamber volume
$v_{r_1}^{(1)}$	velocity of contact point in its relative motion *over* the external gear profile in S1
$\boldsymbol{v}_r^{(1)}$	velocity of contact point in its relative motion *over* the external gear profile
$v_{r_1}^{(2)}$	velocity of contact point in its relative motion *over* the internal gear profile in S1
$\boldsymbol{v}_r^{(2)}$	velocity of contact point in its relative motion *over* the internal gear profile
v_s	sliding velocity modulus
$\boldsymbol{v}_{tr}^{(1)}$	contact point velocity in its transfer motion *with* the external gear profile
$\boldsymbol{v}_{tr}^{(2)}$	contact point velocity in its transfer motion *with* the internal gear profile
ε	flow ripple index
ϕ	generalized parameter of motion
ϕ_i	angular position of external(i=1) or internal (i=2) gear
κ_2	curvature of the internal gear profile
θ	angle between unit vector $\boldsymbol{j}$ 1 and unit normal
$\rho_K^{(i)}$	vector ray connecting rotor (i=1,2) center to two consecutive contact points
ρ	radius of generating pin circle
Σ_i	pin circle (i=1) or pin parabola (i=2) internal gear teeth profile
Σ_1'	envelope to the family curves Σ 2
$\omega_i^{(k)}$	angular velocity of external (k=1) or internal gear (k=2) in S *i*
$\omega_i^{(12)}$	angular velocity in relative motion of body 1 with respect to body 2 in S *i*

Acknowledgements

This work is funded within a research contract between Magneti Marelli SpA Divisione Componenti Meccanici and Dipartimento di Energetica, Politecnico di Torino.

References

Beard, J. E. 1985. *Kinematic analysis of gerotor type pumps, engines and compressors*, Ph. D. dissertation, Purdue University, pp. 108-111.

Beard, J. E. et al. 1989. *The effects of the design parameters on the generated curvature and displacement of epitrochoidal gerotor pumps.* SAE 891831.

Colbourne, J. R. 1976. Reduction of the contact stress in Internal pumps, *Transaction of the ASME J. For Industrial engineering*, Nov. pp. 1296-1300.

Fabiani, M. and Mancò, S. and Nervegna, N. and Rundo, M. et al. 1999. *Modelling and simulation of Gerotor Gearing in Lubricating Oil Pump*. SAE paper 1999-01-0626

Litvin, F. L. 1994. *Gear geometry and applied theory*, Prentice Hall, Englewood Cliffs, N.J..

Litvin, F. L. and Feng, P. H. 1996. Computerized design and generation of cycloidal gearings, *Mech. Mach. Theory*, Vol. 31, No. 7, pp. 891-911.

Mancò, S. and Nervegna, N. and Rundo, M., et al. 1998. Gerotor Lubricating Oil Pump for IC Engines, SAE Paper 982689, *International Fall Fuels & Lubricants Meeting and Exposition*, San Francisco, USA and SAE Transactions.

Mancò, S. and Nervegna, N. and Rundo, M. 1999. Influenza della velocità di rotazione sulcomportamento delle pompe di lubrificazione dei motori a combustione interna, 54° *Congresso Nationale ATI*, 14-17 settembre, L'Aquila, Italy.

Rundo, M. and Mancò, S. and Nervegna, N. 1998. Studio e simulazione di pompe di lubrificazione per impieghi automobilistici, *Magneti Marelli-Politecnico di Torino contracts*, Torino, Italy.

Singh, T. 1991. *Design of vane pump suction porting to reduce cavitation at high operation speeds*. SAE 911937.

Salvatore Mancò
Graduated in Mechanical Engineering at Politecnico di Torino in 1980. His scientific career started on diesel fuels quality, SI engine supercharging and control, and landed, in the 2nd half of the eighties, on fluid power. S. Mancò main contribution to the Fluid Power Scientific community is on the gear pump field. Since 1992, he is associate professor of Energy Systems at Politecnico di Torino.

Nicola Nervegna
Graduated in Nuclear Engineering (1971) from Politecnico di Torino, Italy. He joined the Politecnico staff in October 1971 and, at present, is Professor of Fluid Power Systems. His research interests lie in the broad fields of Fluid Power with involvement in positive displacement pumps as well in the modelling, simulation and testing of various hydraulic components.

Giuseppe Mancò
Graduated in Civil Engineering (1982) from Università degli Studi dell'Aquila. Since 1984 he is professor of applied mathematics at the State Technical Institute in Avezzano. His research interests are focused on differential geometry, tensor analysis and stiff differential equations.

Massimo Rundo
Graduated in Mechanical Engineering at the Politecnico di Torino in 1996. After graduation he participated within the Fluid Power Group of the Politecnico di Torino, as a Magneti Marelli visiting researcher, to an extensive and ongoing research project on gerotor and external gear pumps for internal combustion engines lubrication. He is very active in modelling, simulation and testing of fluid power components.